



---

## Figures and figure supplements

*Hox*-dependent coordination of mouse cardiac progenitor cell patterning and differentiation

**Sonia Stefanovic et al**

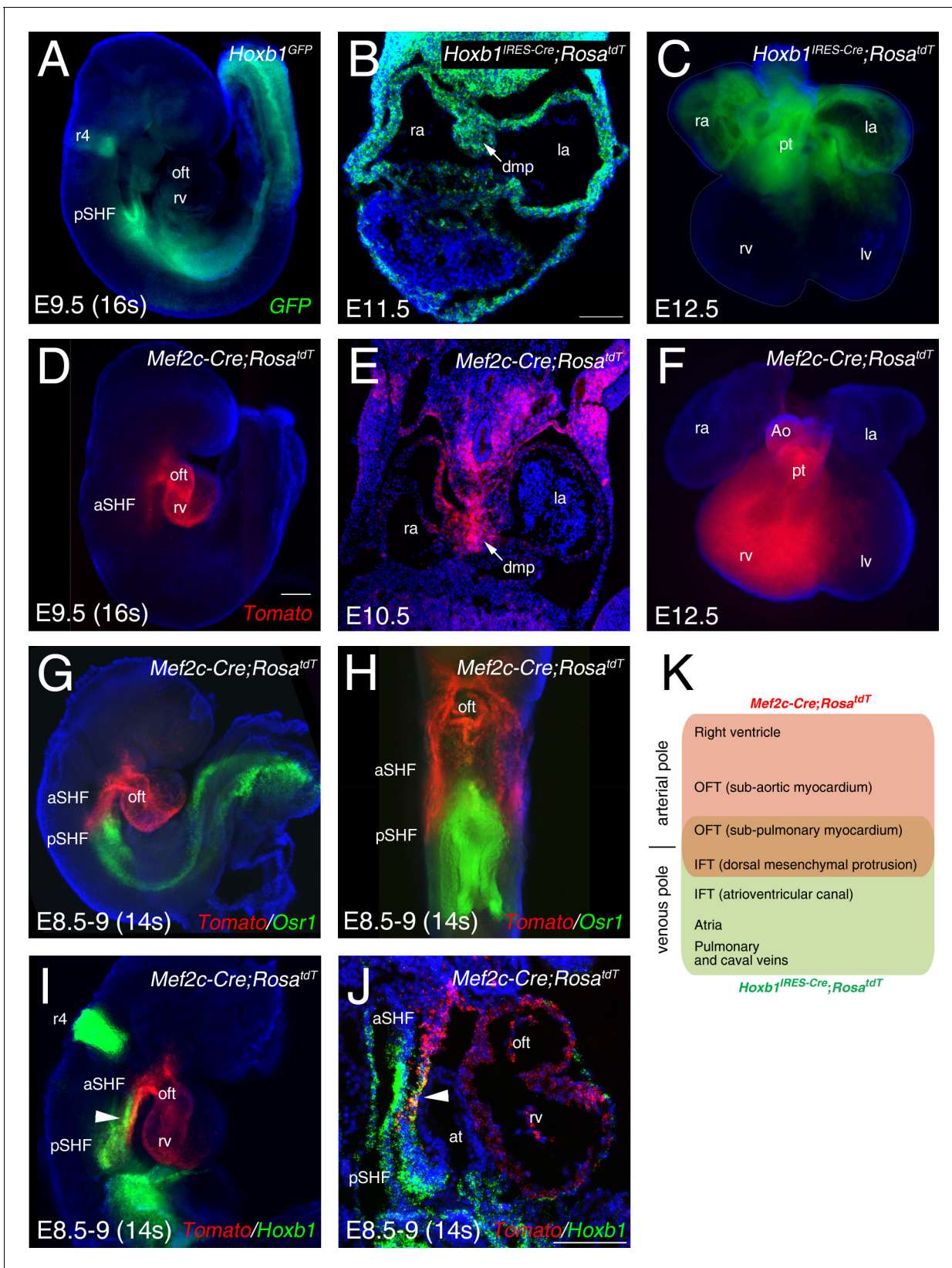
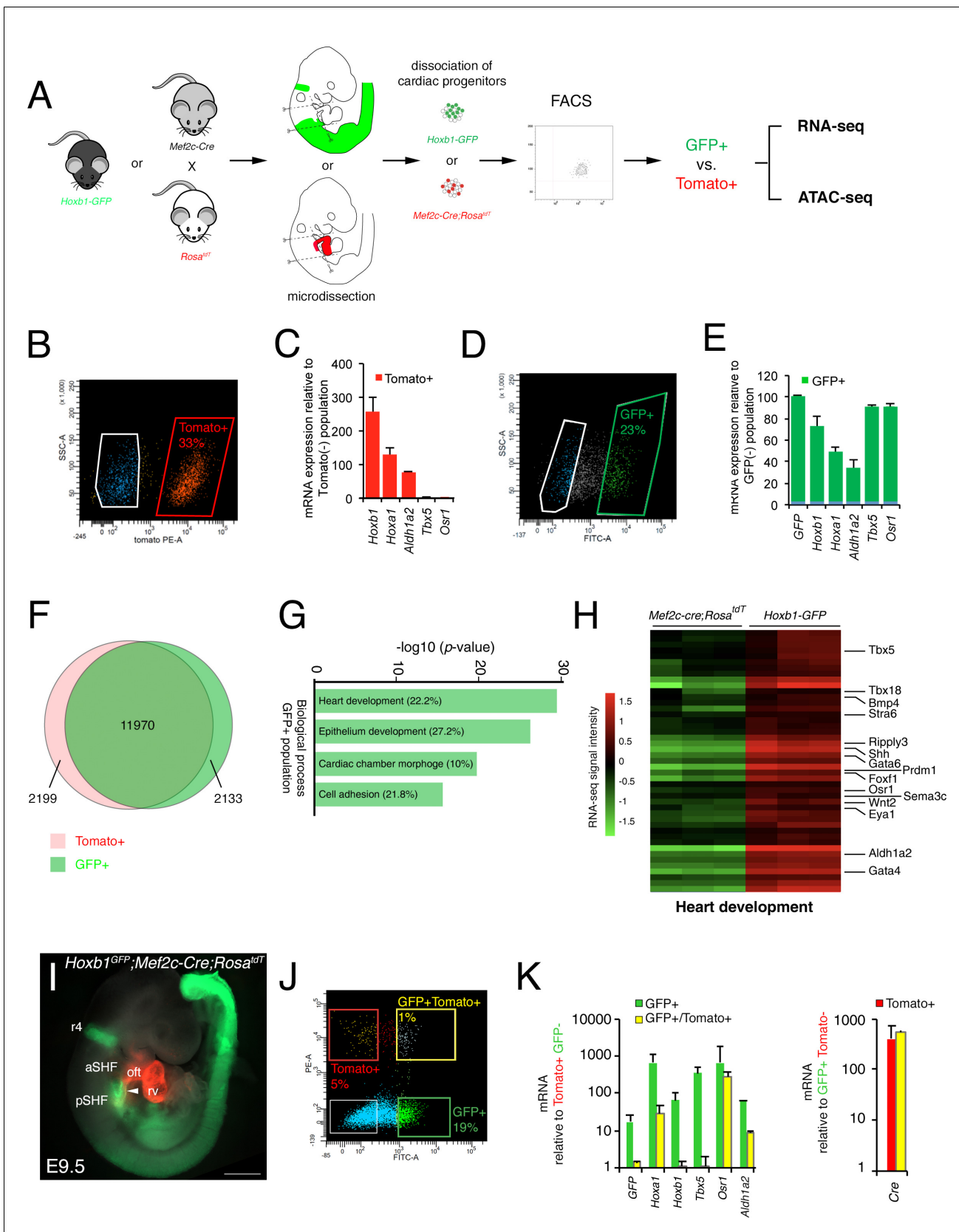


**Figure 1.** Characterization of two transgenic lines defining complementary domains of the SHF. (A) Whole-mount fluorescence microscopy of E9.5 (16 somites [s]) *Hoxb1*<sup>GFP</sup> embryos. (B) Transverse section at E11.5 heart showing *Hoxb1*-Cre genetic lineage contribution to atrial myocardium and the

Figure 1 continued on next page

## Figure 1 continued

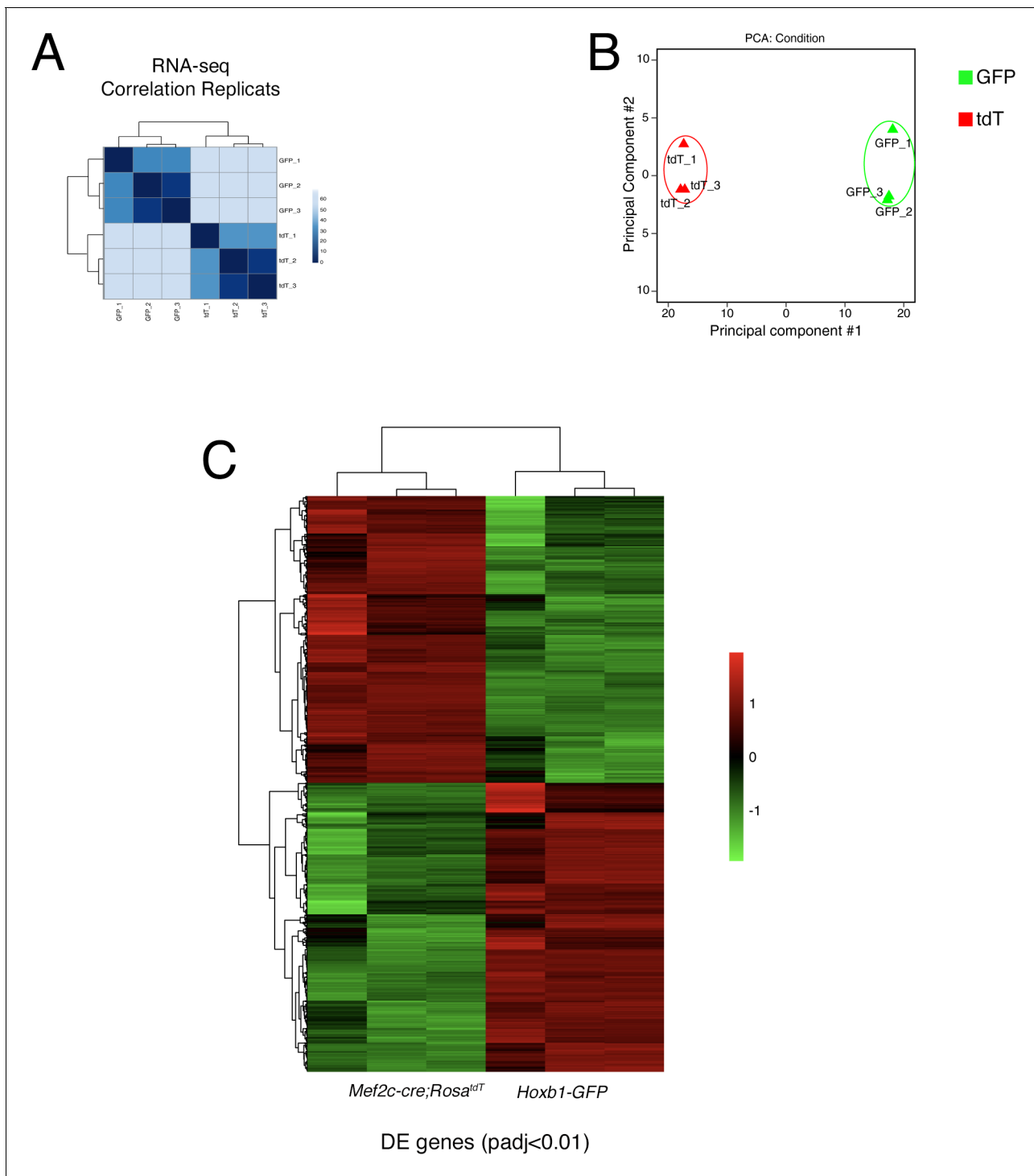
dorsal mesenchymal protrusion (DMP). (C) Ventral view of an E12.5 heart showing the *Hoxb1-Cre* (*Hoxb1<sup>IRE5-Cre</sup>;Rosa<sup>tdT</sup>* - green) genetic lineage contributions to both atria and sub-pulmonary myocardium. (D) E9.5 (16s) *Mef2c-Cre;Rosa<sup>tdT</sup>* embryos showing the contribution of the *Mef2c-Cre* genetic lineage (*Tomato*, red) to the outflow tract and the right ventricle. (E) Transverse section at E10.5 showing the *Mef2c-Cre* genetic lineage contribution to the DMP. (F) Ventral view of an E12.5 heart showing the *Mef2c-Cre* genetic lineage contribution to the right ventricle and great arteries. (G) RNA-FISH showing the expression of *Osr1* (green) and the *Mef2c-Cre* labeled cells (*Tomato*; red). (H) Ventral view of the embryo shown in G. Distribution of *Osr1* is detected in the posterior domain of *Mef2c-Cre*. (I,J) RNA-FISH showing a small domain of overlap between *Hoxb1* (green) and *Mef2c-Cre* labeled cells (*Tomato*; red). (K) Cartoon summarizing the contribution of the *Hoxb1-Cre* (green) and *Mef2c-Cre* (red) lineages in the embryo at E9.5. Nuclei are stained with Hoechst. ao, aorta; at, atria; aSHF, anterior second heart field; ift, inflow tract; la, left atria; lv, left ventricle; oft, outflow tract; pt, pulmonary trunk; pSHF, posterior second heart field; r4, rhombomere 4; ra, right atria; rv, right ventricle; Scale bars represent 100  $\mu\text{m}$  (C, J); 200  $\mu\text{m}$  (D).



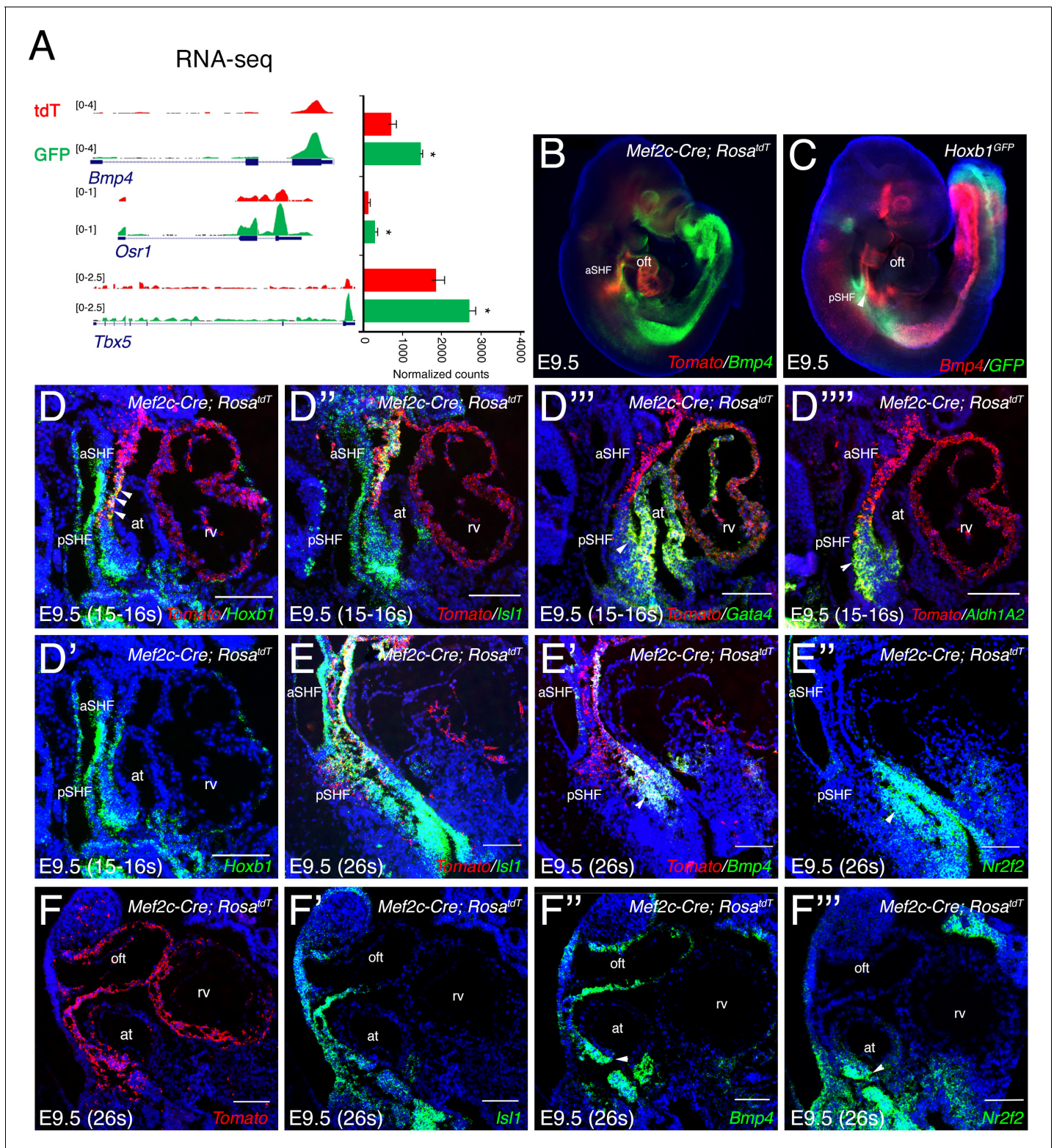
**Figure 2.** Molecular signature of the posterior SHF. (A) Scheme of the protocol utilized to characterize the molecular signature of the SHF on isolated *Mef2c-Cre;Rosa<sup>tdT</sup>* (Tomato) and *Hoxb1<sup>GFP</sup>* (GFP) positive cells. (B,D) FACS profile of E9.5 cardiac progenitor cells isolated from *Mef2c-Cre;Rosa<sup>tdT</sup>* and *Hoxb1<sup>GFP</sup>*. *Figure 2 continued on next page*

## Figure 2 continued

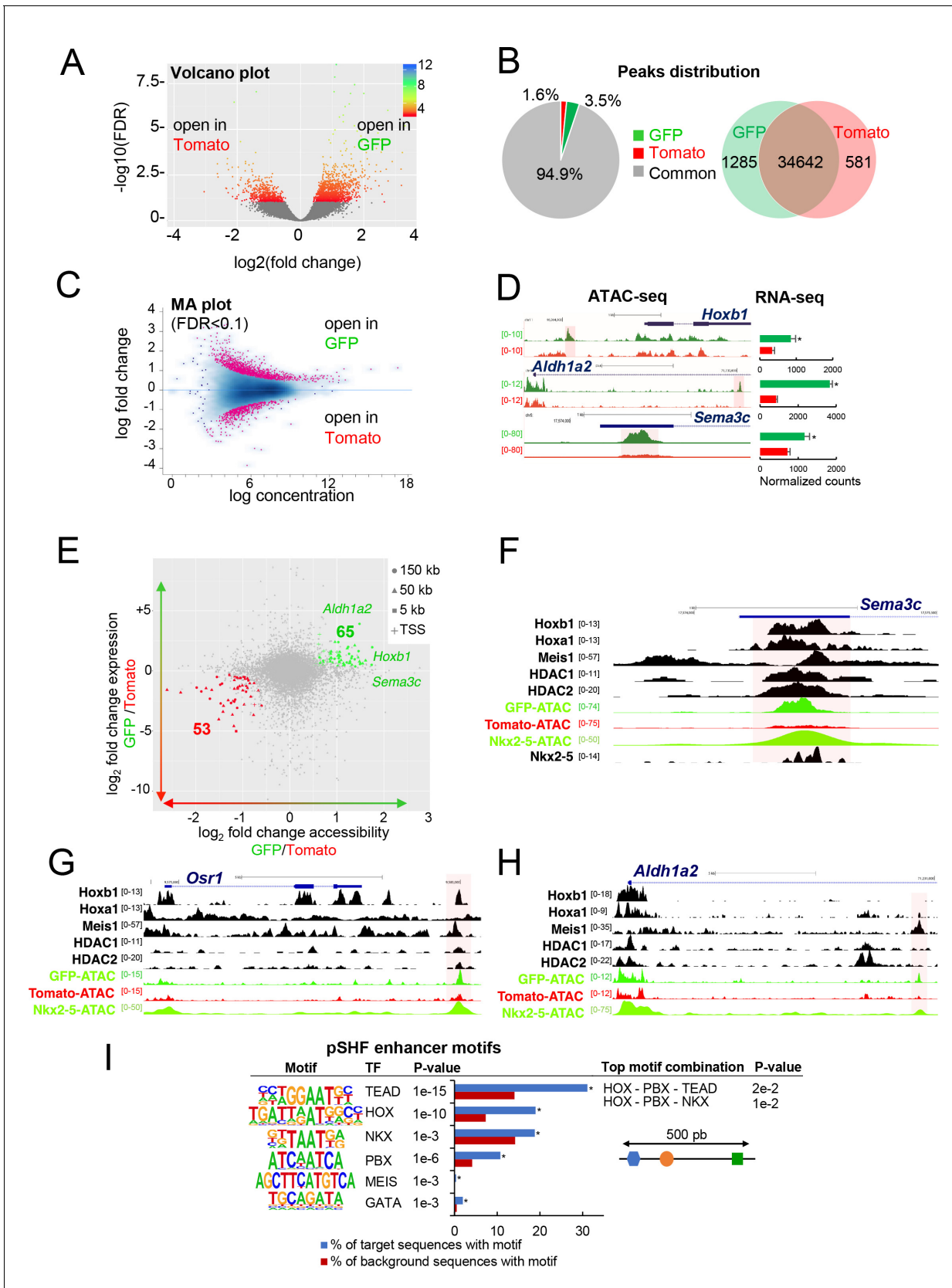
*Hoxb1<sup>GFP</sup>* embryos. (C,E) Expression of pSHF markers (*Hoxa1*, *Hoxb1*, *Osr1*, *Aldh1a2*, *Tbx5*, *GFP*) was analyzed by real-time qPCR. Data were normalized to *HPRT* and expressed as folds of increase over negative population. (F) Venn diagram showing transcripts differentially expressed in the GFP+ (green) compared to the Tomato+ (red) populations. (G) Gene ontology (GO) analysis of GFP+ progenitor cells performed with ClusterProfiler system showing enrichment of upregulated genes in the pSHF with ranked by  $-\log_{10}$  (p-value). The percentage corresponds to the 'BG ratio' obtained in the GO analysis. (H) Example of the heatmap of 'heart development' GO term associated genes analyzed by RNA-seq (n = 3 from GFP+ cells, n = 3 from Tomato+ cells). (I) Whole-mount fluorescence microscopy of triple transgenic *Hoxb1<sup>GFP</sup>;Mef2c-Cre;Rosa<sup>tdT</sup>* embryos at stage E9.5. (J) FACS profile of E9.5 cardiac progenitor cells isolated from *Hoxb1<sup>GFP</sup>;Mef2c-Cre;Rosa<sup>tdT</sup>* embryos. (K) Expression of pSHF markers (*Hoxa1*, *Hoxb1*, *Osr1*, *Aldh1a2*, *Tbx5*), *GFP* and the *Cre* recombinase were analyzed with real-time qPCR. Data were normalized to *HPRT* and expressed as folds of increase over negative population. aSHF, anterior SHF; oft, outflow tract; pSHF, posterior SHF; rv, right ventricle. Scale bars: 500  $\mu$ m.



**Figure 2—figure supplement 1.** Quality assessment of RNA-seq data performed with purified cardiac progenitor cells. (A) Replicate correlation for RNA-seq datasets from GFP+ and Tomato+ progenitor cells. (B) Principal component analysis (PCA) of RNA-sequencing datasets from GFP+ and Tomato+ progenitor cells. (C) Unsupervised hierarchical clustering of all differentially expressed genes between GFP+ and Tomato+ progenitor cells.



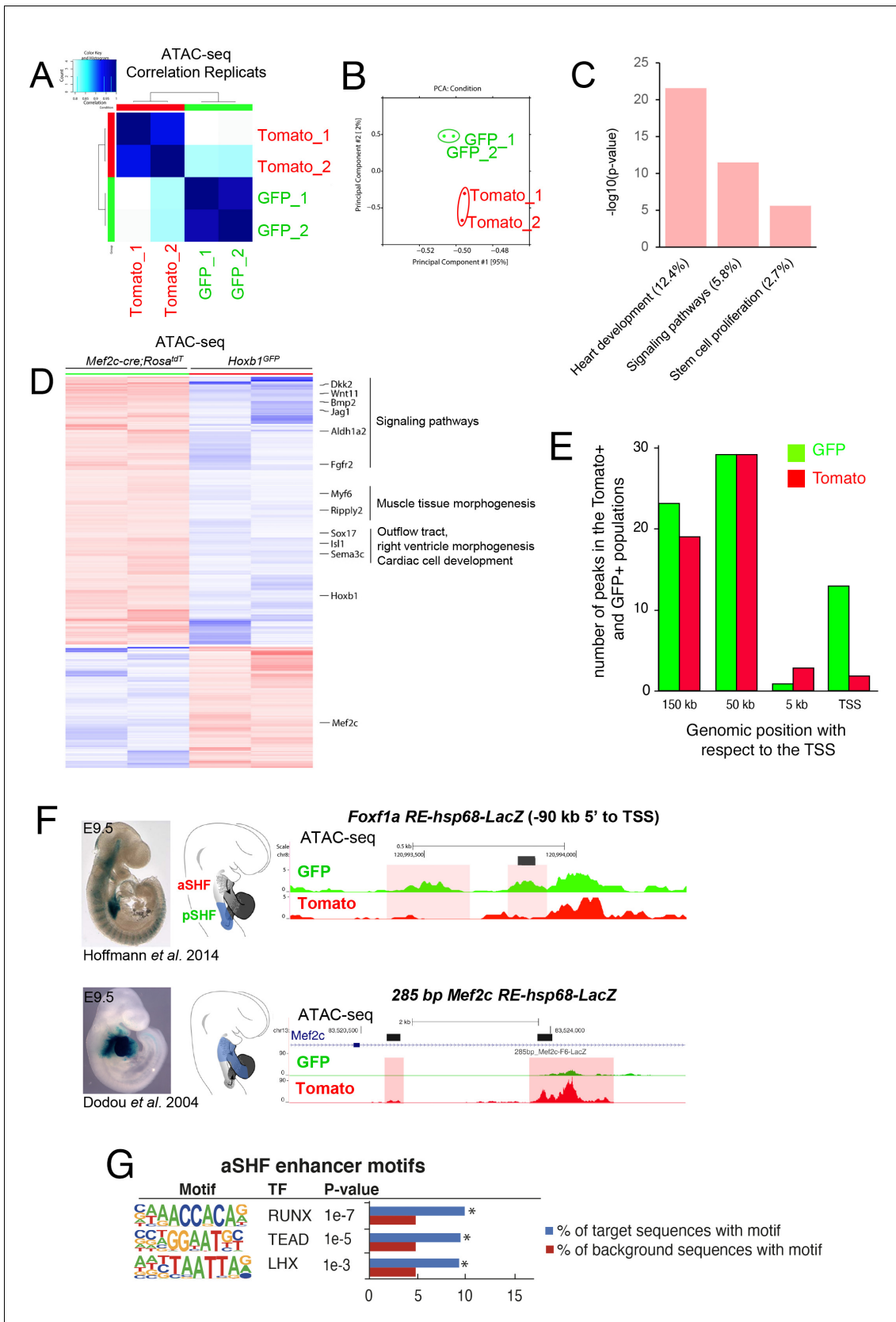
**Figure 2—figure supplement 2.** Spatial validation of marker gene expression in cardiac progenitor populations. (A) RNA-sequencing datasets visualized for the pSHF markers *Tbx5*, *Osr1* and *Bmp4*. (B) Whole-mount RNA-FISH analysis showing the distribution of *Bmp4* transcript (green) in cells overlapping with the posterior border of *Mef2c-Cre* lineage contribution (red). (C) *Bmp4* (red) is expressed in the pSHF overlapping with *Hoxb1-GFP* (green; arrowhead). (D–F) RNA-FISH analysis on serial sagittal sections of *Mef2c-Cre; Rosa<sup>tdT</sup>* embryos, showing expression of genes enriched in the GFP+ progenitor population (E and F are from the same embryo). *Hoxb1*, *Gata4*, *Aldh1a2* and *Nr2f2* mark the pSHF, whereas *Bmp4* expression is enriched in the pSHF compared to the aSHF. Scale bars: 100  $\mu$ m.



**Figure 3.** Differential chromatin accessibility in GFP+ and Tomato+ cardiac progenitor cells. (A) Volcano plot of ATAC-seq performed from GFP+ and Tomato+ cardiac progenitors. (B) Pie chart showing the distribution of the ATAC-seq peaks in the two populations. Venn diagram showing overlap of Figure 3 continued on next page

## Figure 3 continued

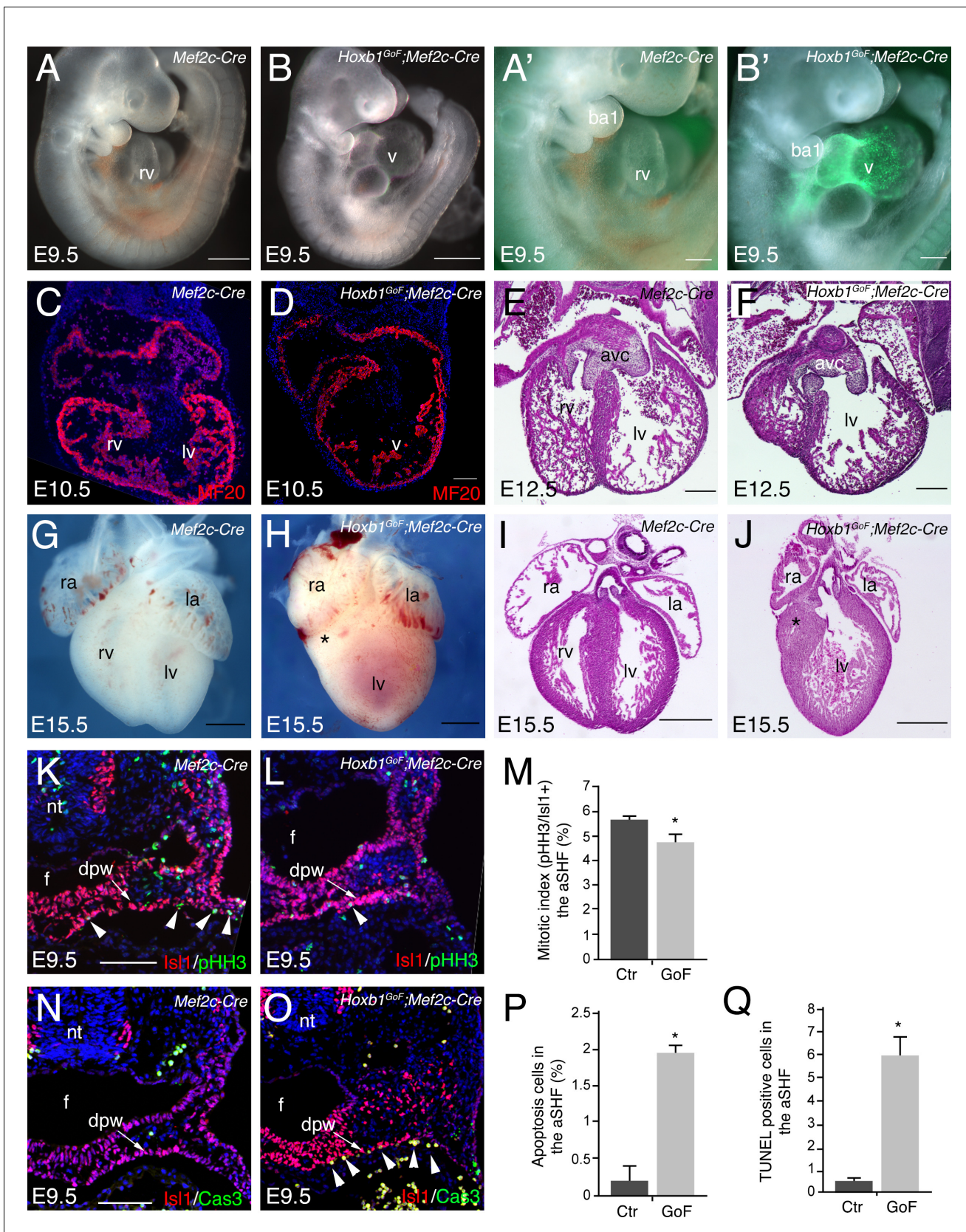
the ATAC-seq peaks in the two populations. (C) MA plot of ATAC-seq peaks in GFP+ versus Tomato+ cells. (D) Open chromatin profiles correlate with transcriptional expression. Browser views of *Hoxb1*, *Aldh1a2* and *Sema3c* loci with ATAC-seq profiles of GFP+ pSHF progenitor cells (green) and Tomato+ *Mef2c-Cre* labeled cells (red). Data represent merged technical and biological replicates for each cell type. The y-axis scales range from 0 to 80 in normalized arbitrary units. The tracks represent ATAC-seq, whereas the bar graphs represent RNA-seq. Boxed regions show cell-type-specific peaks around *Aldh1a2*, *Osr1*, and *Sema3C* gene loci. (E) Change in accessibility versus change in gene expression in GFP+ and Tomato+ cells. For each ATAC-seq peak, the log of the ratio of normalized ATAC-seq reads (GFP/Tomato) is plotted on the x-axis, and the log of the ratio normalized RNA-seq reads corresponding to the nearest gene is plotted in the y-axis. Peaks that are both significantly differentially accessible (FDR < 0.1) and significantly differentially expressed (FDR < 0.1) are colored green (more open in GFP+ cells, higher expression in GFP+ cells; 65 peaks) or red (more open in Tomato population, higher expression in Tomato; 53 peaks). (F–H) Browser views of *Sema3c* (F), *Osr1* (G) and *Aldh1a2* (H) gene loci with ATAC-seq profiles of GFP+ pSHF progenitor cells (green) and Tomato+ *Mef2c-Cre* labeled cells (red). Open chromatin profiles correlate with transcription factor binding at putative enhancers specific for cardiac progenitor cells. (I) pSHF enhancers were enriched in DNA binding motifs for HOX and known cardiac transcription factors such as PBX and MEIS. HOX recognition motifs were strongly enriched in a known motif search in pSHF enhancers. Other enriched matrices match binding sites of known cardiac regulators. HOX binding motifs are highly enriched at genomic regions bound by cardiac transcription factors. *p*-values were obtained using HOMER (Heinz et al., 2010). Combinations of 3 sequence motifs contained within 500 bp are shown.



**Figure 3—figure supplement 1.** Quality assessment of ATAC-seq data performed with purified cardiac progenitor cells. (A) Replicate correlation for ATAC-seq datasets from GFP+ and Tomato+ progenitor cells. (B) Principal component analysis (PCA) of ATAC-sequencing datasets from GFP+ and Tomato+ progenitor cells. (C) Enrichment of biological pathways in ATAC-seq datasets. (D) ATAC-seq signal for *Mef2c* and *Hoxb1* in *Mef2c-cre:Rosa<sup>tdT</sup>* and *Hoxb1<sup>GFP</sup>* mice. (E) ATAC-seq signal for *Mef2c* and *Hoxb1* in *Mef2c-cre:Rosa<sup>tdT</sup>* and *Hoxb1<sup>GFP</sup>* mice. (F) ATAC-seq signal for *Foxf1a* and *Mef2c* in *Foxf1a RE-hsp68-LacZ* and *Mef2c RE-hsp68-LacZ* mice. (G) aSHF enhancer motifs. *Figure 3—figure supplement 1 continued on next page*

*Figure 3—figure supplement 1 continued*

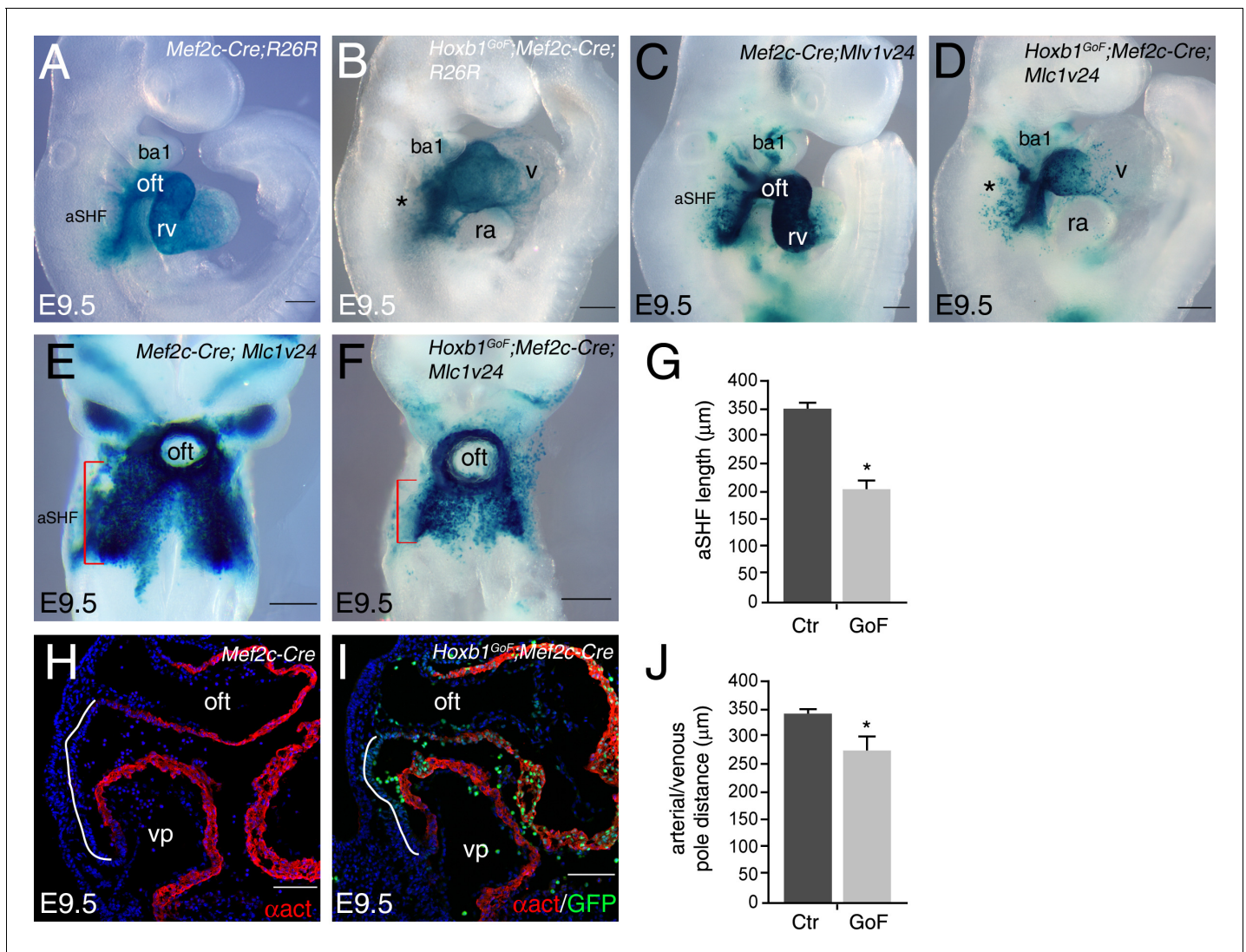
Tomato+ progenitor cells. (C) The Gene Ontology (GO) analysis results for the gene loci harboring peaks strictly present in the GFP+ population. (D) Heat maps show the ATAC-seq enrichment ( $\pm 150$  kb region upstream from the annotated TSS). (E) Histograms showing the number of ATAC-seq peaks in the two populations regarding their genomic position with respect to the TSS. (F) ATAC-sequencing on SHF cells identifies previously established SHF REs for *Foxf1a* (top) and *Mef2c* (bottom). (G) aSHF enhancers are enriched in DNA binding motifs for RUNX and TEAD transcription factors. *p*-values were obtained using HOMER (Heinz et al., 2010).



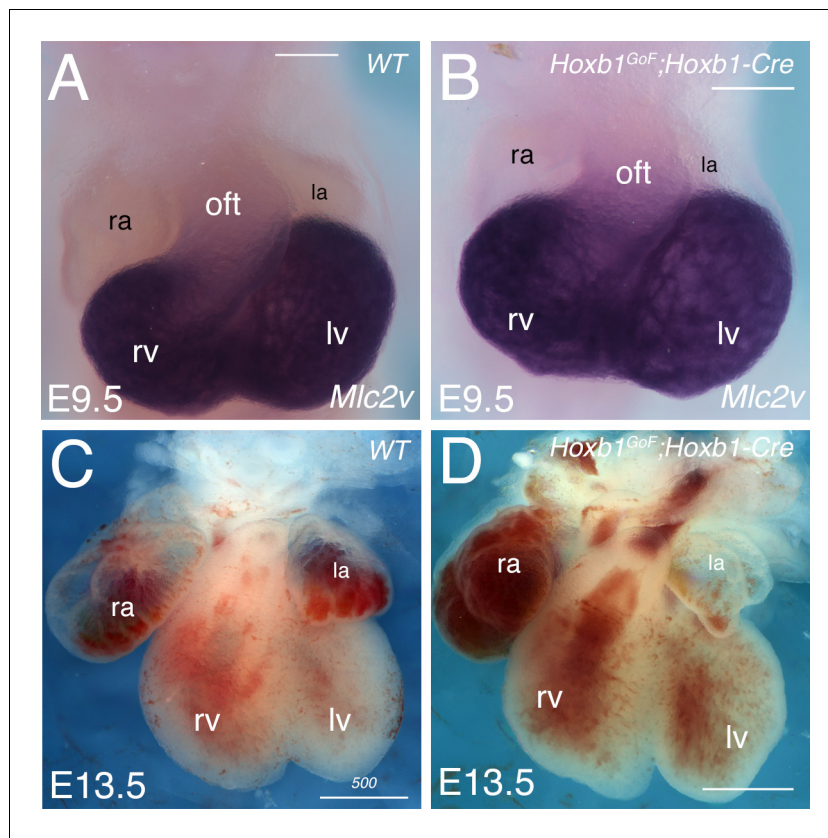
**Figure 4.** Activation of *Hoxb1* expression in aSHF progenitors disrupts the formation of the right ventricle. (A,B) Macroscopic view of *Mef2c-AHF-Cre* (*Mef2c-Cre*, control) and *Hoxb1<sup>GoF</sup>;Mef2c-Cre* embryos at E9.5. (A',B') High magnification of embryo in A and B showing GFP activity in the Cre-  
 Figure 4 continued on next page

## Figure 4 continued

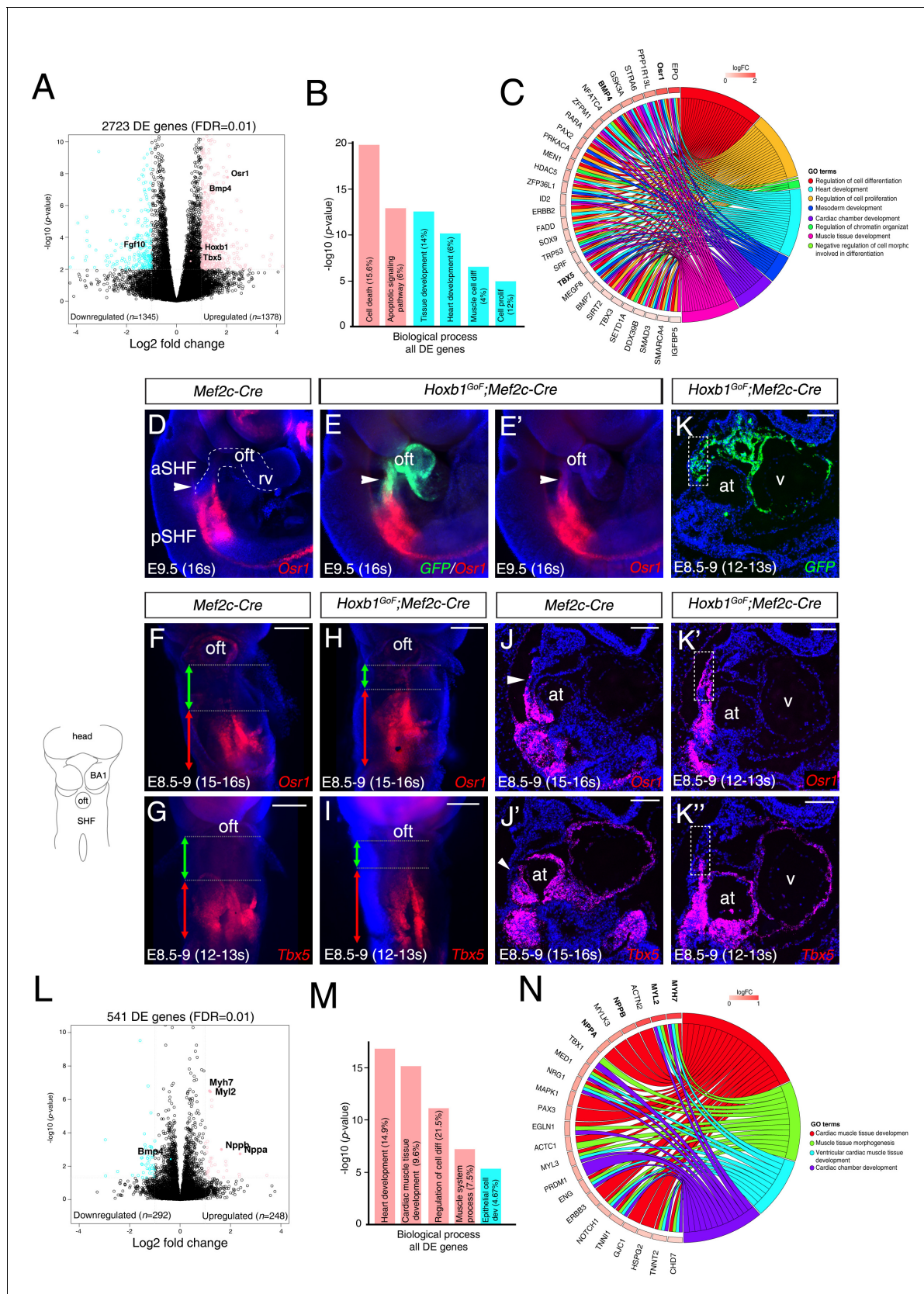
recombinase driven cells. (C,D) Immunofluorescence with MF20 (red) in control (C) and *Hoxb1<sup>GoF</sup>;Mef2c-Cre* (D) hearts at E10.5. (E–J) Hematoxylin and Eosin (H and E) staining on transversal section of control (E,I) and *Hoxb1<sup>GoF</sup>;Mef2c-Cre* (F,J) hearts at E12.5 and E15.5. The right ventricle (asterisk) in *Hoxb1<sup>GoF</sup>;Mef2c-Cre* hearts is hypoplastic compared to control hearts (n = 8). (G,H) Whole-mount views of control (G) and *Hoxb1<sup>GoF</sup>;Mef2c-Cre* (H) hearts at E15.5. (K,L) Immunofluorescence with *Isl1* (red) and Phospho-histone H3 (pHH3, green) on *Mef2c-Cre* (K) and *Hoxb1<sup>GoF</sup>;Mef2c-Cre* (L) embryos at E9.5. (M) Quantification of pHH3-positive cells in the aSHF *Isl1*<sup>+</sup>, showed a reduced of the mitotic index in *Hoxb1<sup>GoF</sup>;Mef2c-Cre* (n = 3; GoF) compared to *Mef2c-Cre* (Ctr) (n = 7) embryos. (N,O) Immunofluorescence with *Isl1* (red) and Caspase 3 (Cas3, green) on *Mef2c-Cre* (N) and *Hoxb1<sup>GoF</sup>;Mef2c-Cre* (O) embryos at E9.5. Arrowheads indicate Cas3-positive cells. (P) Quantification of Cas3-positive cells revealed increased cell death in the aSHF of *Hoxb1<sup>GoF</sup>;Mef2c-Cre* embryos. (Q) Quantification of TUNEL staining performed on *Mef2c-Cre* (Ctr) and *Hoxb1<sup>GoF</sup>;Mef2c-Cre* embryos (GoF). ao, aorta; avc, atrioventricular canal; ba, branchial arch; dpw, dorsal pericardial wall; f, foregut pocket; la, left atrium; lv, left ventricle; nt, neural tube; oft, outflow tract; PM, pharyngeal mesoderm; pt, pulmonary trunk; ra, right atrium; rv, right ventricle. Scale bars: 100  $\mu$ m (A',B',D,E,F); 200  $\mu$ m (A',B',E,F); 500  $\mu$ m (A,B,G–J).



**Figure 4—figure supplement 1.** Reduction of SHF length in *Hoxb1<sup>GoF</sup>;**Mef2c-Cre* embryos. (A–F) X-gal staining of control and *Hoxb1<sup>GoF</sup>;**Mef2c-Cre* embryos carrying out *R26R* (A,B) or *Mlc1v24* (C–F) transgenes at E9.5. (A,B) Anterior SHF is disrupted in *Hoxb1<sup>GoF</sup>;**Mef2c-Cre* embryos. (E,F) X-gal staining showing anterior SHF in *Mef2c-Cre*;*Mlc1v24* (control; E) and *Hoxb1<sup>GoF</sup>;**Mef2c-Cre*;*Mlc1v24* (F) embryos at E9.5. (G) Measurement of staining revealed a decrease of anterior SHF length in *Hoxb1<sup>GoF</sup>;**Mef2c-Cre*;*Mlc1v24* compared to control embryos. (H,I) Immunofluorescence with  $\alpha$ -actinin ( $\alpha$  act, red) and GFP (green) on *Mef2c-Cre* (control; H) and *Hoxb1<sup>GoF</sup>;**Mef2c-Cre* (I) embryos at E9.5. (J) Measurement of distance between arterial and venous poles reveals a reduction of dorsal pericardial wall length in *Hoxb1<sup>GoF</sup>;**Mef2c-Cre* embryos. All measures were calculated from  $n = 6$  embryos for each genotype. Histograms are expressed as mean  $\pm$  SEM.  $p$ -values were determined by Student's  $t$  test. (\* $p < 0.01$ ). Scale bars: 100  $\mu\text{m}$  (H,I) and 200  $\mu\text{m}$  (A–D,E,F).



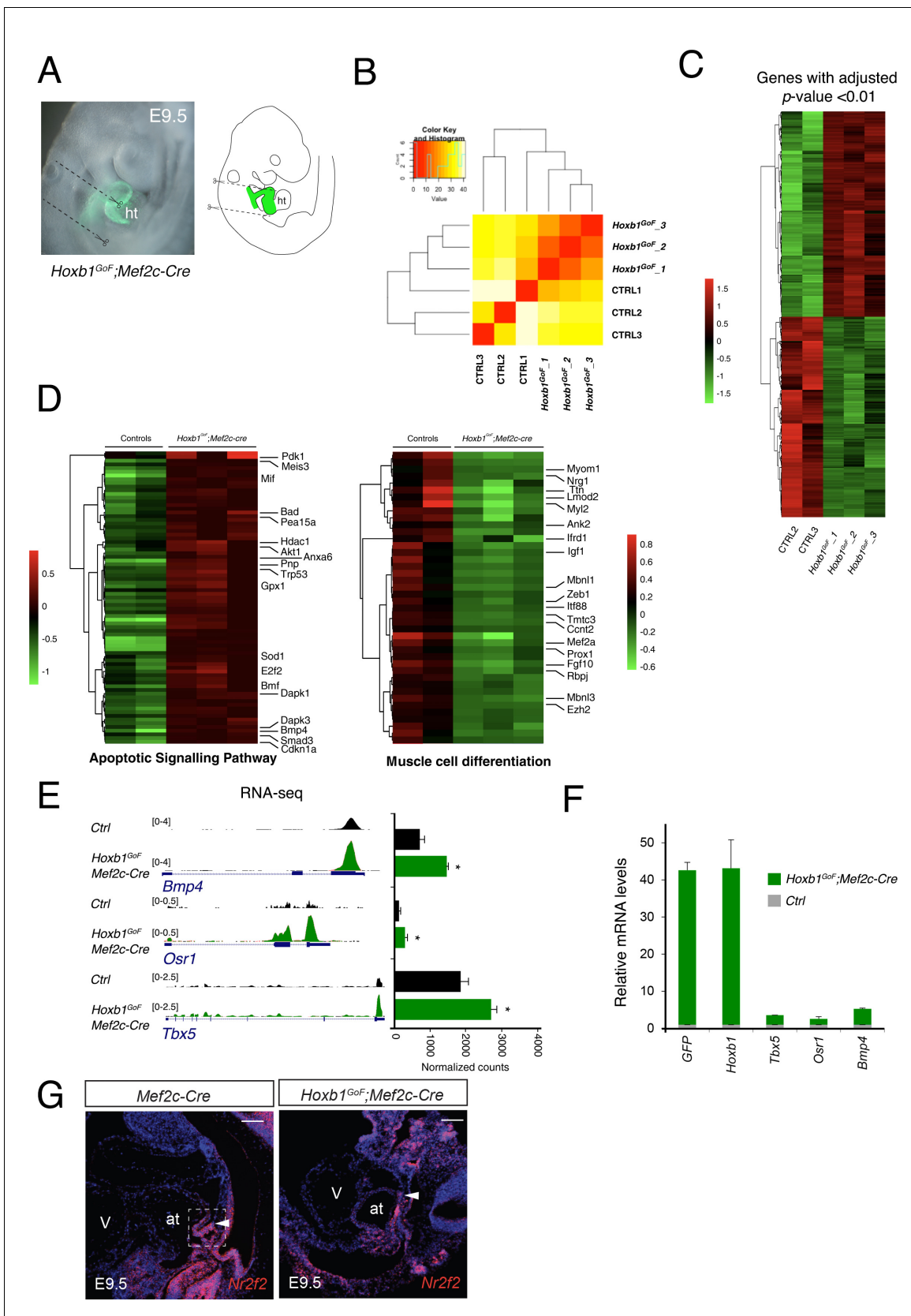
**Figure 4—figure supplement 2.** Over-expression of *Hoxb1* in the pSHF does not affect the morphology of the embryonic heart. (A,B) Whole-mount in situ hybridization with *Mlc2v* riboprobe on E9.5 wild-type (WT; A) and *Hoxb1<sup>GoF</sup>;**Hoxb1-Cre* (B) embryos. Hearts are similar in WT and *Hoxb1<sup>GoF</sup>;**Hoxb1-Cre* embryos. (C,D) Frontal views of wild-type (WT; A), and *Hoxb1<sup>GoF</sup>;**Hoxb1-Cre* (D) hearts at E13.5. No obvious anomalies are detected in *Hoxb1<sup>GoF</sup>;**Mef2c-Cre* embryos. la, left atria; lv, left ventricle; oft, outflow tract; ra, right atria; rv, right ventricle. Scale bars: 200 μm (A,B) and 500 μm (C,D).



**Figure 5.** *Hoxb1* regulates progenitor identity and differentiation in the pSHF. (A) Volcano plot of transcriptional profiling results with significantly dysregulated genes between *Hoxb1<sup>GoF</sup>;Mef2c-Cre* and control SHF. The y-axis corresponds to the mean expression value of  $\log_{10}$  (p-value), and the x-axis corresponds to the  $\log_2$  fold change. Figure 5 continued on next page

## Figure 5 continued

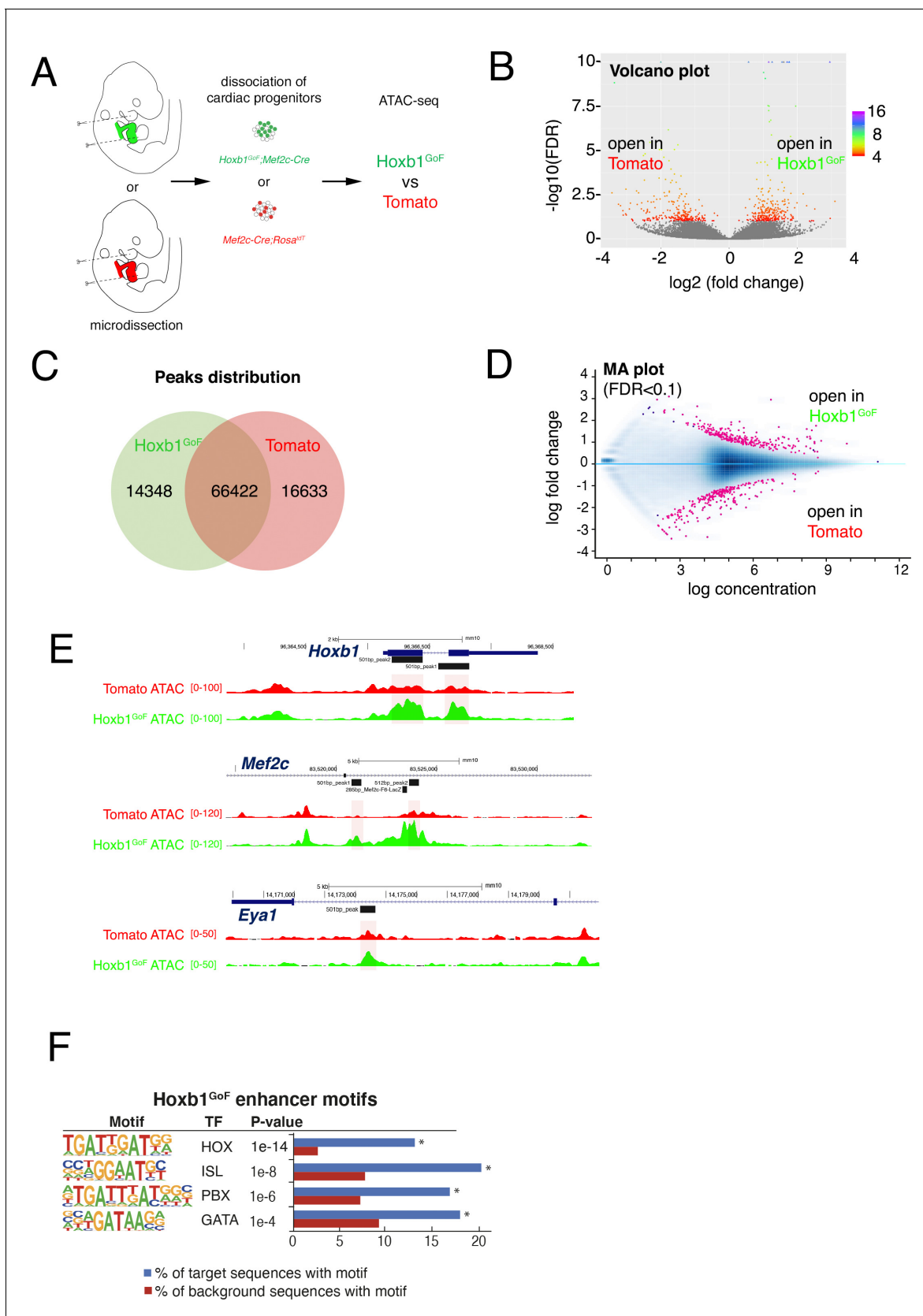
axis displays the log<sub>2</sub> fold change value. The colored dots represent the significantly differential expressed transcripts ( $p < 0.05$ ); the black dots represent the transcripts whose expression levels did not reach statistical significance ( $p > 0.05$ ). Differential expression analysis performed using DESeq2 revealed 2,723 genes with Log<sub>2</sub>-fold changes  $\geq 1$  at a False Discovery Rate (FDR)  $\leq 0.01$ . (B) Gene ontology (GO) analysis of genes deregulated in *Hoxb1<sup>GoF</sup>;Mef2c-Cre* embryos performed with ClusterProfiler system. The percentage corresponds to the 'BG ratio' obtained in the GO analysis. (C) Chord plot showing a selection of genes upregulated in *Hoxb1<sup>GoF</sup>;Mef2c-Cre* embryos present in the represented enriched GO terms. Outer ring shows log<sub>2</sub> fold change or GO term grouping (right, key below). Chords connect gene names with GO term groups. (D) Whole-mount RNA-FISH for *Osr1* on E9.5 *Mef2c-Cre* embryos in lateral views. (E, E') Whole-mount RNA-FISH for *GFP* (green) and *Osr1* (red) on E9.5 *Hoxb1<sup>GoF</sup>;Mef2c-Cre* embryos. Whole-mount RNA-FISH for *Osr1* in ventral views (F, H) and *Tbx5* (G, I) on E8.5-9 *Mef2c-Cre* and *Hoxb1<sup>GoF</sup>;Mef2c-Cre* embryos. An anteriorly shifted expression of *Osr1* and *Tbx5* is detected in *Hoxb1<sup>GoF</sup>;Mef2c-Cre* embryos compared to their control littermates (same somite stage – 15-16s for *Osr1* and 12-13s for *Tbx5*). RNA-FISH against *Osr1*, *Tbx5* and *GFP* on serial sections in *Hoxb1<sup>GoF</sup>;Mef2c-Cre* embryos (K, K', K'') compared to control littermates (J, J'; Serial sagittal sections). (L) Volcano plot showing differential expressed genes between *Hoxb1<sup>-/-</sup>* and wild-type samples. The y-axis corresponds to the mean expression value of log<sub>10</sub> ( $p$ -value), and the x-axis displays the log<sub>2</sub> fold change value. Colored dots represent the significantly differential expressed transcripts ( $p < 0.05$ ); the black dots represent the transcripts whose expression levels did not reach statistical significance ( $p > 0.05$ ). We identified 249 genes upregulated, and 292 genes downregulated in *Hoxb1<sup>-/-</sup>* embryos. (M) GO analysis of genes deregulated in *Hoxb1<sup>-/-</sup>* embryos with ranked by  $-\log_{10}$  ( $p$ -value). (N) Chord plot showing a selection of genes upregulated in dissected pharyngeal mesoderm of *Hoxb1<sup>-/-</sup>* embryos present in the represented enriched GO terms. Outer ring shows log<sub>2</sub> fold change or GO term grouping (right, key below). Chords connect gene names with GO term groups. Nuclei are stained with Hoechst. at, atria; BA1, branchial arch 1; oft, outflow tract; SHF, second heart field; V, ventricle. Scale bars: 200  $\mu$ m (F, G, H, I); 100  $\mu$ m (J, J', K, K', K'').



**Figure 5—figure supplement 1.** Quality assessment of RNA-seq data performed on the *Hoxb1<sup>GoF</sup>;Mef2c-Cre* embryos. (A) Macroscopic view of *Hoxb1<sup>GoF</sup>;Mef2c-Cre* embryos at E9.5 and the micro-dissected region comprising the SHF progenitors and excluding the forming heart. (B) Replicate Figure 5—figure supplement 1 continued on next page

## Figure 5—figure supplement 1 continued

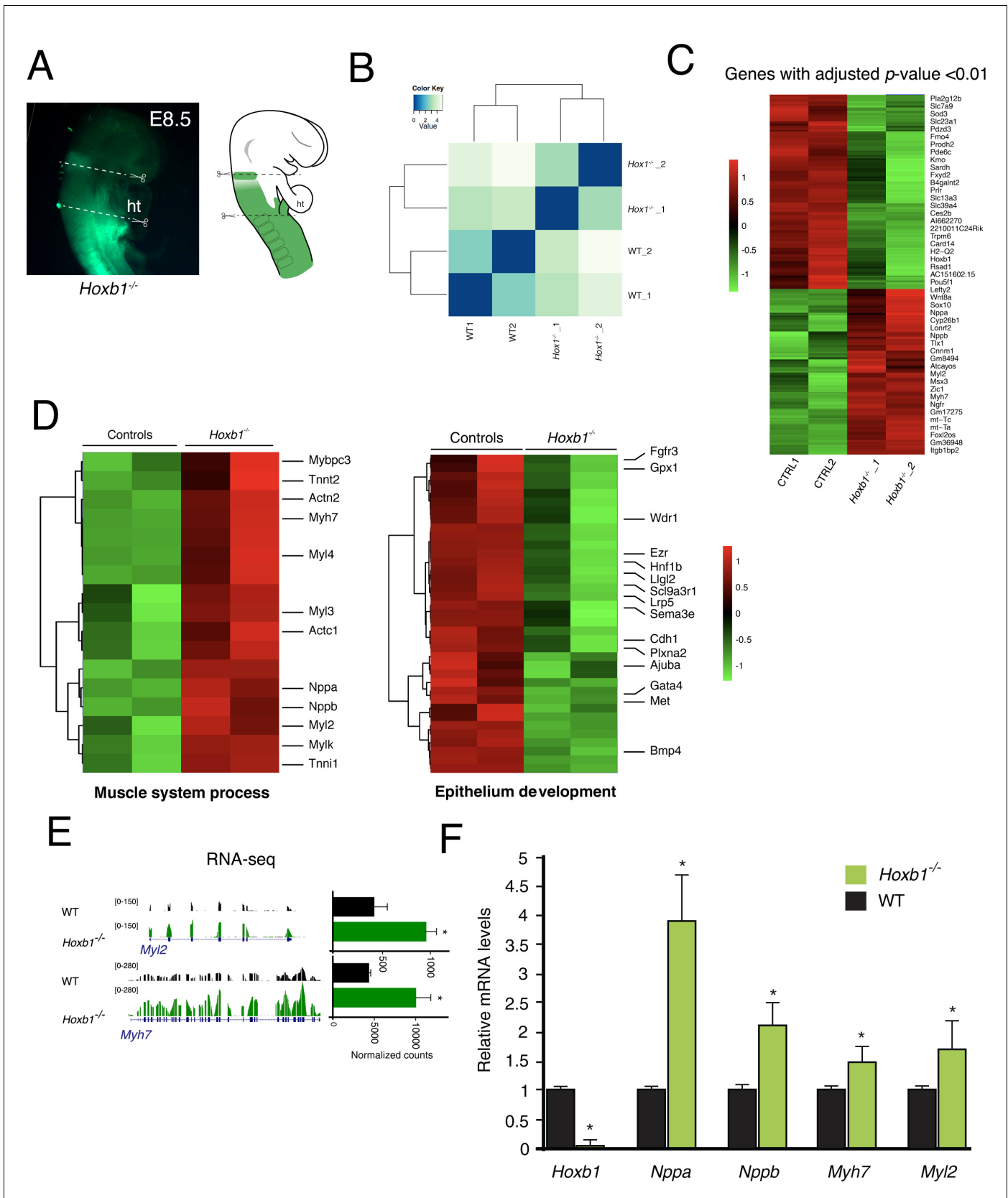
correlation for RNA-seq datasets from *Hoxb1<sup>GoF</sup>;Mef2c-Cre* (GoF) and control (Ctrl) regions. (C) Unsupervised hierarchical clustering of all differentially expressed genes between GoF and control regions. (D) Heatmap of 'apoptotic signaling pathway' and 'muscle cell differentiation' associated genes analyzed by RNA-seq. (e) RNA-seq datasets visualized for the pSHF markers *Tbx5*, *Osr1* and *Bmp4*. (F) Real time PCR validation of RNA-seq results. Data were normalized to HPRT and expressed as fold increase over control samples. (G) RNA-FISH against *Nr2f2* (red) on section of E9.5 *Mef2c-Cre* (control) and *Hoxb1<sup>GoF</sup>;Mef2c-Cre* embryos. An anterior shift in expression of *Nr2f1* is detected in *Hoxb1<sup>GoF</sup>;Mef2c-Cre* compared to control embryos. Nuclei are stained with Hoechst. at, atria; V, ventricle. Scale bars: 200  $\mu$ m.



**Figure 5—figure supplement 2.** Chromatin accessibility when *Hoxb1* is ectopically expressed in the *Mef2c-Cre*<sup>+</sup> cardiac progenitor cells. (A) Schemes of *Hoxb1<sup>GoF</sup>;Mef2c-Cre* (GFP<sup>+</sup> named *Hoxb1<sup>GoF</sup>*) and *Mef2c-Cre;Rosa<sup>tdT</sup>* (Tomato<sup>+</sup>) embryos at E9.5 and the micro-dissected regions (GFP<sup>+</sup> or Tomato) Figure 5—figure supplement 2 continued on next page

Figure 5—figure supplement 2 continued

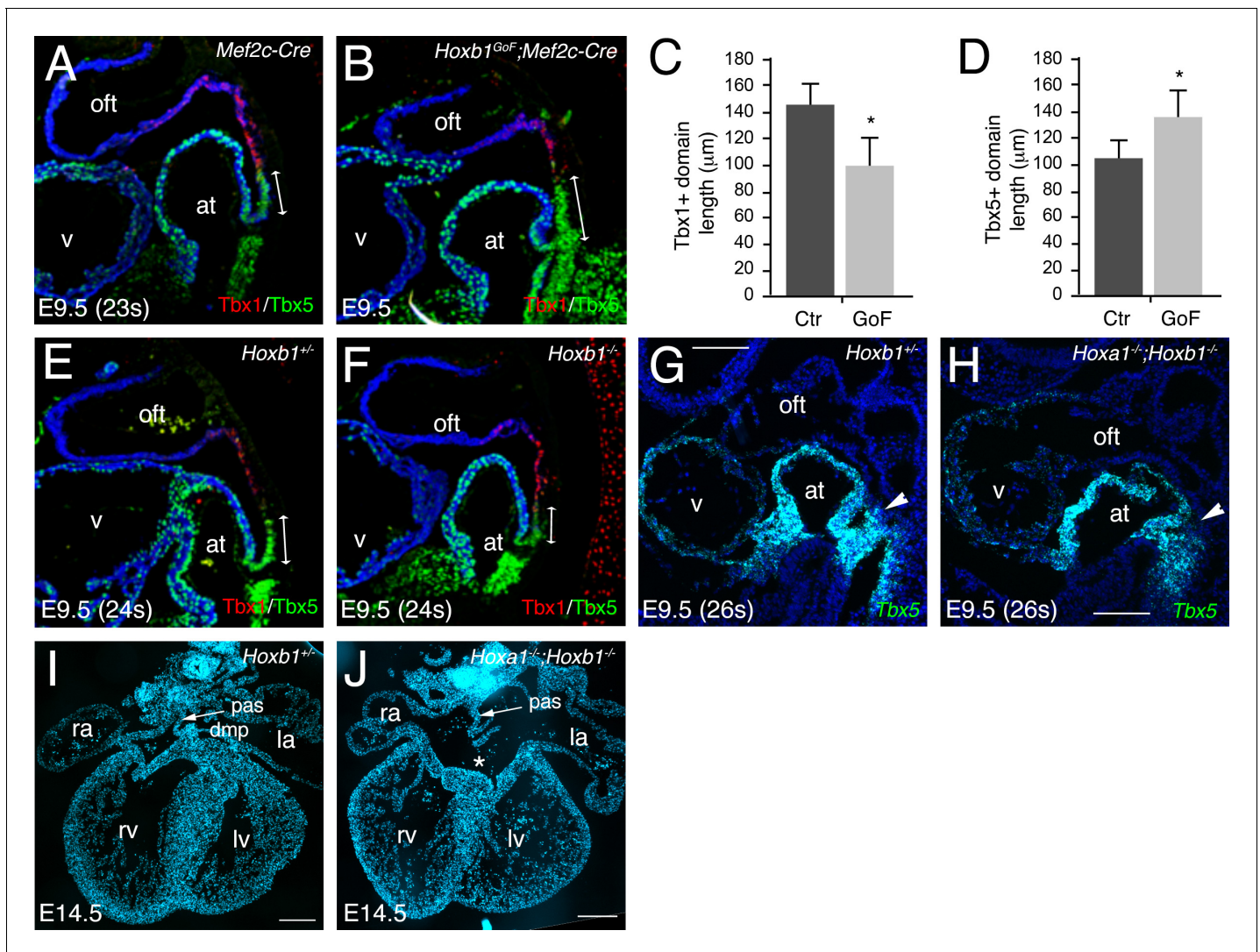
+) comprising aSHF progenitors and the outflow tract of the forming heart. (B) Volcano plot of ATAC-seq performed from *Hoxb1*<sup>GoF</sup> and Tomato+ cells. (C) Venn diagram showing overlap of the ATAC-seq peaks in the two populations. (D) MA plot of ATAC-seq peaks in *Hoxb1*<sup>GoF</sup> versus Tomato+ cells. (E) Open chromatin profiles correlate with transcriptional expression. Browser views of *Hoxb1*, *Mef2c* and *Eya1* loci with ATAC-seq profiles of *Hoxb1*<sup>GoF</sup> cells (green) and Tomato+ *Mef2c-Cre;Rosa<sup>tdT</sup>* labeled cells (red). Data represent merged technical and biological replicates for each cell type. The y-axis scales range from 0 to 100; 0–120 and 0–50 in normalized arbitrary units. The tracks represent ATAC-seq data. Boxed regions show cell-type-specific peaks around *Hoxb1*, *Mef2c*, and *Eya1* gene loci. (F) *Hoxb1*<sup>GoF</sup> enhancers were enriched in DNA binding motifs for HOX and known cardiac transcription factors including PBX and GATA factors. HOX recognition motifs were strongly enriched in a known motif search of *Hoxb1*<sup>GoF</sup> enhancers. *p*-values were obtained using HOMER.



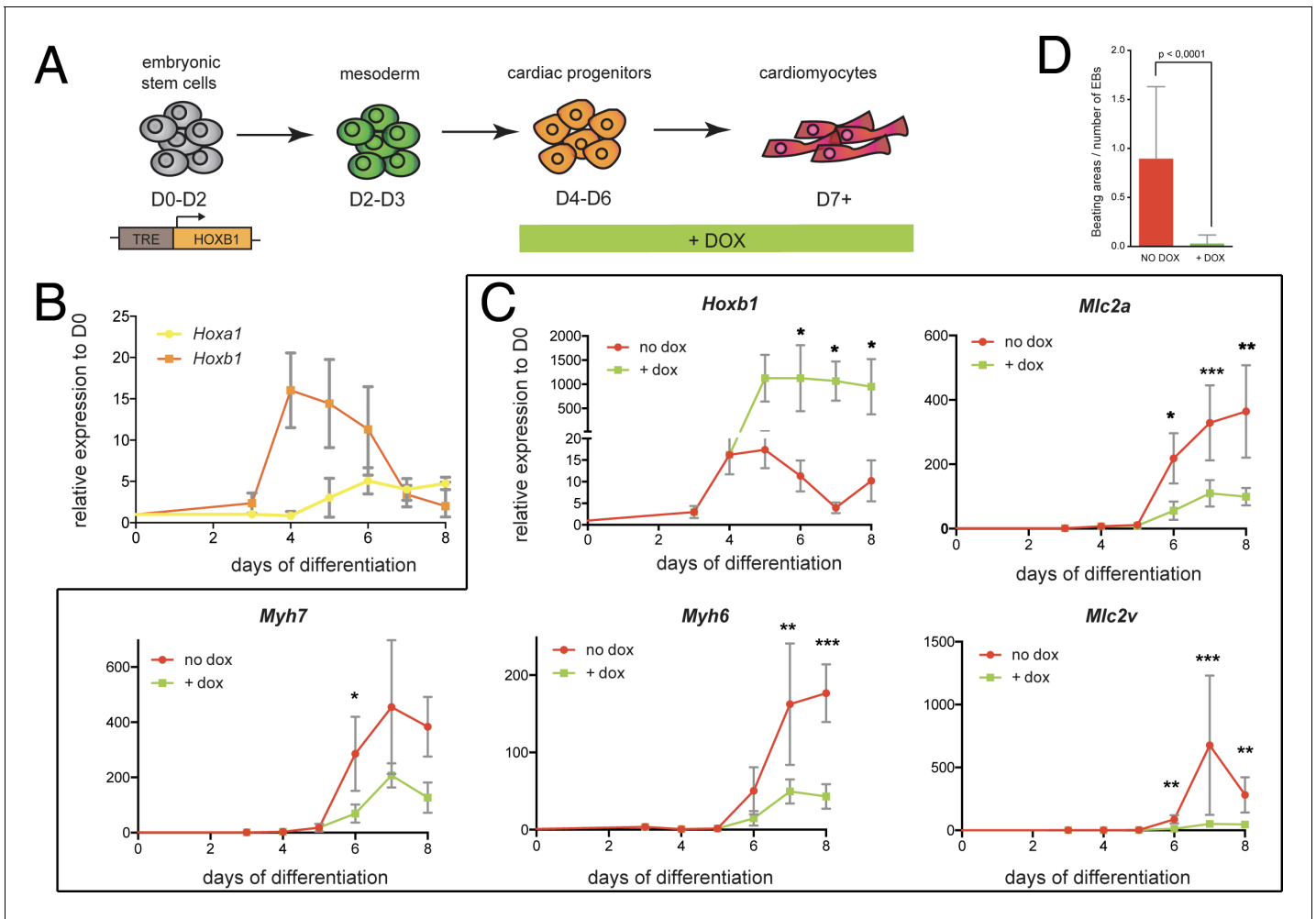
**Figure 5—figure supplement 3.** Quality assessment of RNA-seq data performed on the *Hoxb1*<sup>-/-</sup> embryos. (A) Macroscopic view of *Hoxb1*<sup>-/-</sup> embryos at E8.5 (6-8ps) and the micro-dissected region comprising the SHF progenitors. (B) Replicate correlation for RNA-seq datasets from *Hoxb1*<sup>-/-</sup> and wild-type. Figure 5—figure supplement 3 continued on next page

Figure 5—figure supplement 3 continued

type (WT) regions. (C) Unsupervised hierarchical clustering of all differentially expressed genes between *Hoxb1*<sup>-/-</sup> over WT regions. (D) Heatmap of 'muscle system process' and 'epithelium development' associated genes analyzed by RNA-seq. (E) RNA-sequencing datasets visualized for the cardiac differentiation markers *Myf2* and *Myh7*. (F) Real time PCR validation of RNA-seq results. Data were normalized to HPRT and expressed as fold increase over WT samples.



**Figure 6.** *Hoxa1* and *Hoxb1* genes are required for atrioventricular septation. (A–D) Immunofluorescence on medial sagittal sections showing Tbx1 (red) and Tbx5 (green) protein distribution at E9.5 (23–24 s). (A,B) At E9.5, a boundary is observed in *Mef2c-Cre* embryos between Tbx1+ cells close to the arterial pole of the heart and Tbx5+ cells in the pSHF. In *Hoxb1<sup>GoF</sup>;Mef2c-Cre* embryos the Tbx1+ domain appears reduced although the boundary is maintained. (C) Measurement of the Tbx1+ domain confirmed a decrease of aSHF length in *Hoxb1<sup>GoF</sup>;Mef2c-Cre* (GoF) compared to control (Ctr) embryos. (D) Measurement of the Tbx5+ domain revealed a shift of the boundary since the length of the pSHF was increased in *Hoxb1<sup>GoF</sup>;Mef2c-Cre* (GoF) compared to control (Ctr) embryos. (E,F) The Tbx5+ domain appears reduced in *Hoxb1<sup>-/-</sup>* embryos compared to *Hoxb1<sup>+/-</sup>* littermates. (G,H) RNA-FISH on sagittal sections showing the reduction of Tbx5+ domain in the pSHF of *Hoxa1<sup>-/-</sup>;Hoxb1<sup>-/-</sup>* embryos compared to *Hoxb1<sup>+/-</sup>* littermates. (I,J) DAPI stained sections of a *Hoxb1<sup>+/-</sup>* (I) and a *Hoxa1<sup>-/-</sup>;Hoxb1<sup>-/-</sup>* (J) heart at E14.5 showing the primary atrial septum (pas, arrow). Note the AVSD and absence of the DMP in J, n = 3. at, atria; la, left atrium; lv, left ventricle; ra, right atrium; rv, right ventricle; SHF, second heart field; v, ventricle; la, left atrium; lv, left ventricle; ra, right atrium; rv, right ventricle. Scale bars: 100 μm (E,F); 200 μm (G,H).



**Figure 7.** *Hoxb1* overexpression in mES leads to arrested cardiac differentiation. (A) Scheme of the experiment. Using the tet-ON/*Hoxb1* mouse embryonic stem cell line (Gouti and Galvas, 2008), *Hoxb1* expression was induced by addition of 1  $\mu\text{g/ml}$  of doxycycline (DOX) at the cardiac progenitor stage from day 4 (D4) during mES cell differentiation into cardiac cells. (B) Kinetics of *Hoxa1* and *Hoxb1* during mES cell differentiation as measured by real time qPCR. Results are normalized for gene expression in undifferentiated mES cells (D0). (C) Kinetics of expression for *Hoxb1* and *Myh6*, *Myh7*, *Mlc2v* (or *Myl2*), *Mlc2a* during mES cell differentiation after induction of *Hoxb1* expression (+ dox) or in control condition (no dox). Results are normalized for gene expression in undifferentiated mES cells (D0). Paired, one-sided t-test was performed based on relative transcript expression between control (no dox) and doxycycline treatment (+ dox). \* indicates a significance level of  $p < 0.05$ , \*\* indicates  $p < 0.005$ , \*\*\* indicates  $p < 0.0005$ . (D) Quantification of beating areas relative to the number of embryonic bodies (EBs) at D8 of mES cell differentiation with or without doxycycline addition. Error bars indicate mean  $\pm$  SEM;  $n = 4$  experiments.

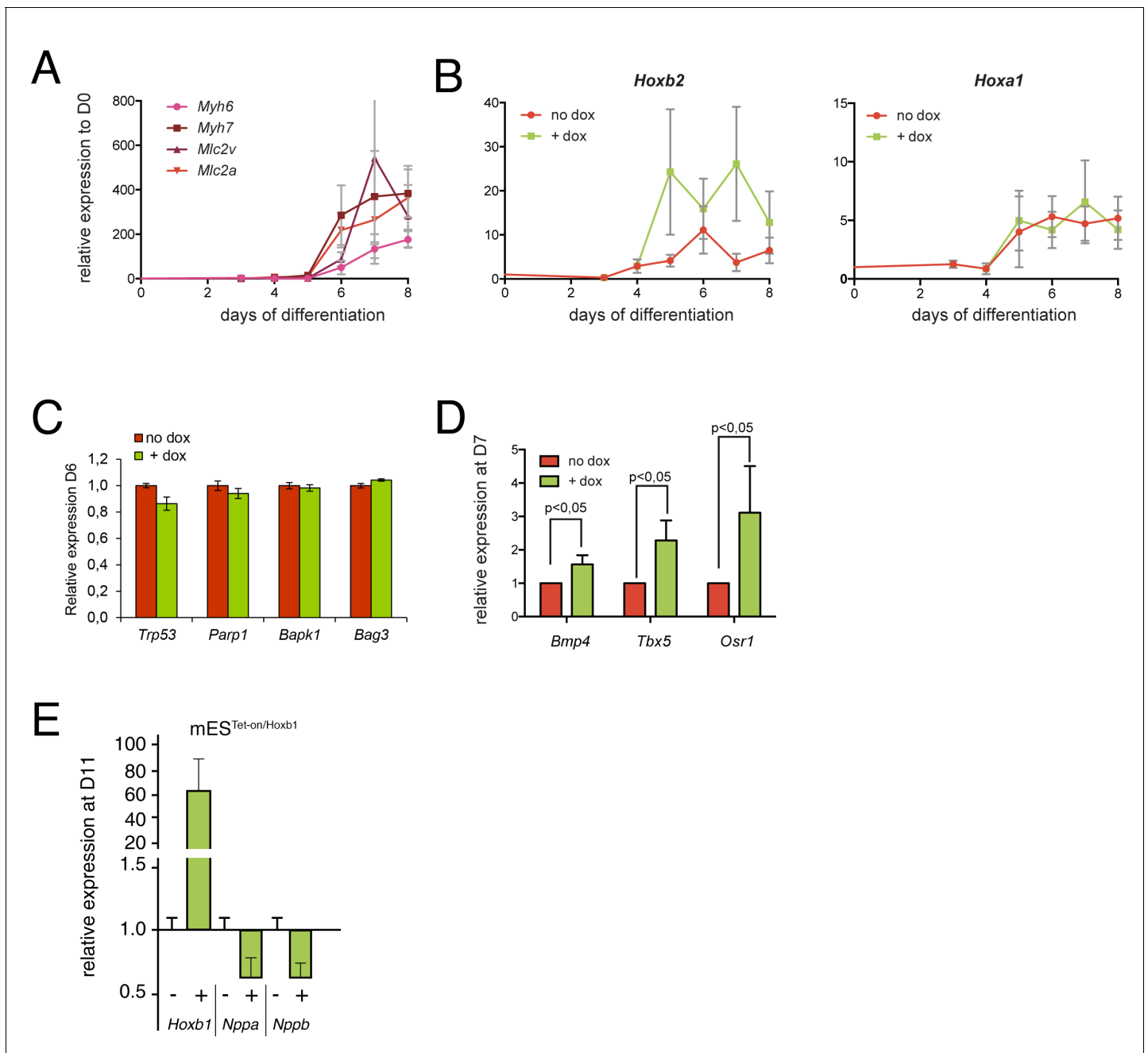


**Figure 7—figure supplement 1.** Expression analysis using the mES cells overexpressing model. (A) Kinetics of myocardial genes (*Myh6*, *Myh7*, *Myh2* (*Mlc2v*), *Mlc2a*) during mES cell differentiation as measured by real time qPCR. (B) Kinetics of *Hoxa1* and *Hoxb2* during mES cell differentiation after induction of *Hoxb1* expression (+ dox) or in control condition (no dox). Results are normalized for gene expression in undifferentiated mES cells (D0). (C) Relative expression of apoptosis genes (*Trp53*, *Parp1*, *Bapk1*, *Bag3*) at D6 of mES cell differentiation as measured by real time RT-PCR in mES cells induced or not for *Hoxb1* expression (+ dox vs no dox). (D) Relative expression of posterior markers of the SHF (*Bmp4*, *Tbx5*, *Osr1*) at D7 of mES cell differentiation as measured by real time PCR in mES cells induced or not for *Hoxb1* expression (+ dox vs no dox). (E) Relative expression of *Hoxb1*, *Nppa* and *Nppb* at D11 of mES cell differentiation as measured by real time RT-PCR in mES cells induced or not for *Hoxb1* expression (+ dox vs no dox). Results are normalized for mRNA expression in untreated cells (no dox). Error bars indicate mean + / - SEM; n = 4 experiments.

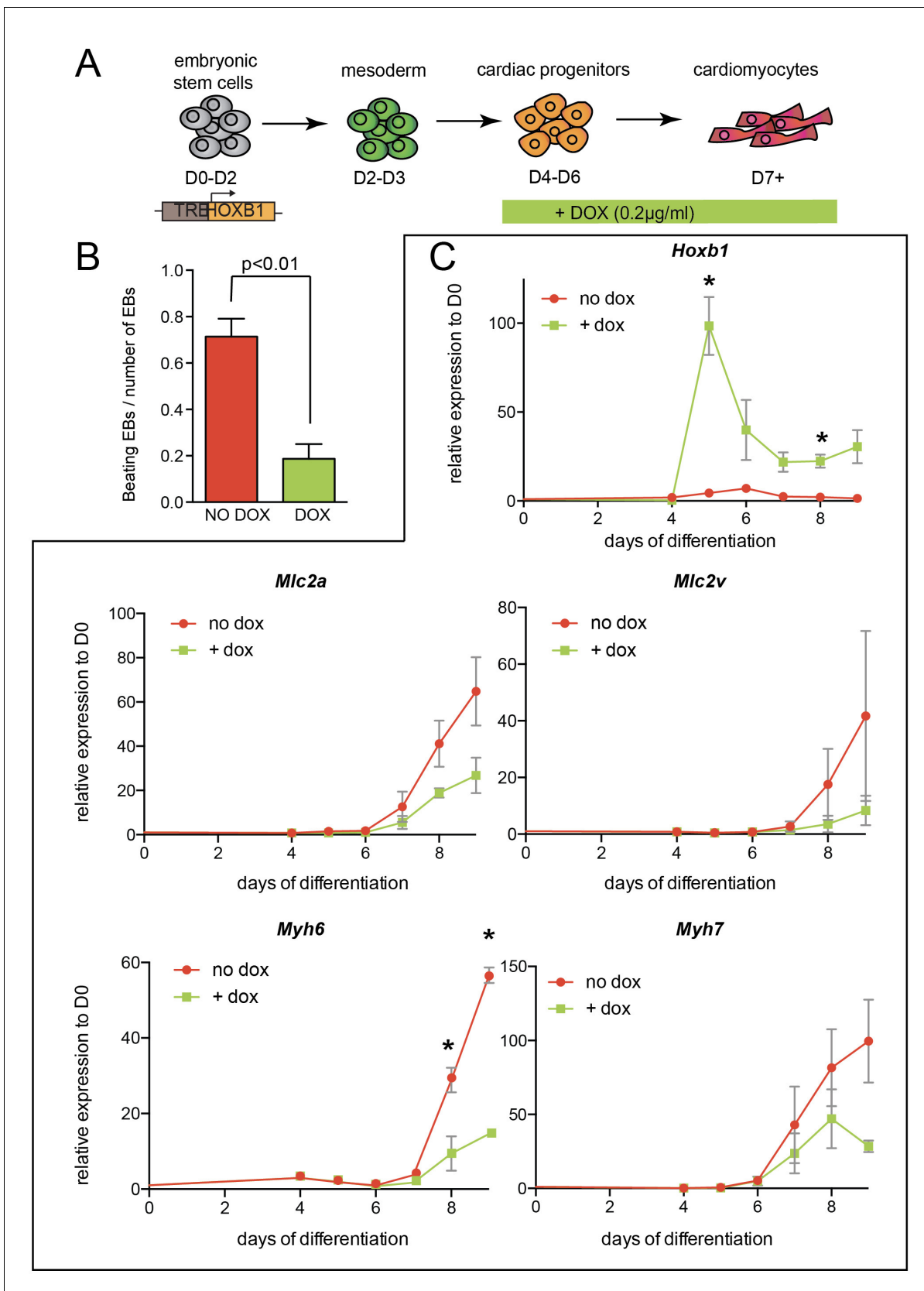


**Figure 7—figure supplement 2.** Arrested cardiac differentiation in mES cells using a lower induction of Hoxb1. (A) Scheme of the experiment. Using the tet-ON/Hoxb1 mouse embryonic stem cell line (Gouti and Gavalas, 2008), Hoxb1 expression was induced by addition of 0.2 µg/ml of doxycycline Figure 7—figure supplement 2 continued on next page

Figure 7—figure supplement 2 continued

(DOX) from day 4 (**D4**) during mES cell differentiation into cardiac cells. (**B**) Quantification of beating embryoid bodies (EBs) relative to the total number of embryoid bodies. (**C**) Kinetics of expression for Hoxb1 and Myh6, Myh7, Mlc2v (or Myl2), Mlc2a during mES cell differentiation after induction of Hoxb1 expression (+ dox) or in control condition (no dox). Results are normalized for gene expression in undifferentiated mES cells (**D0**). Error bars indicate mean + / - SEM; n = 2 experiments. Paired, one-sided t-test was performed based on relative transcript expression between control (no dox) and doxycycline treatment (+ dox). \* indicates a significance level of  $p < 0.05$ .

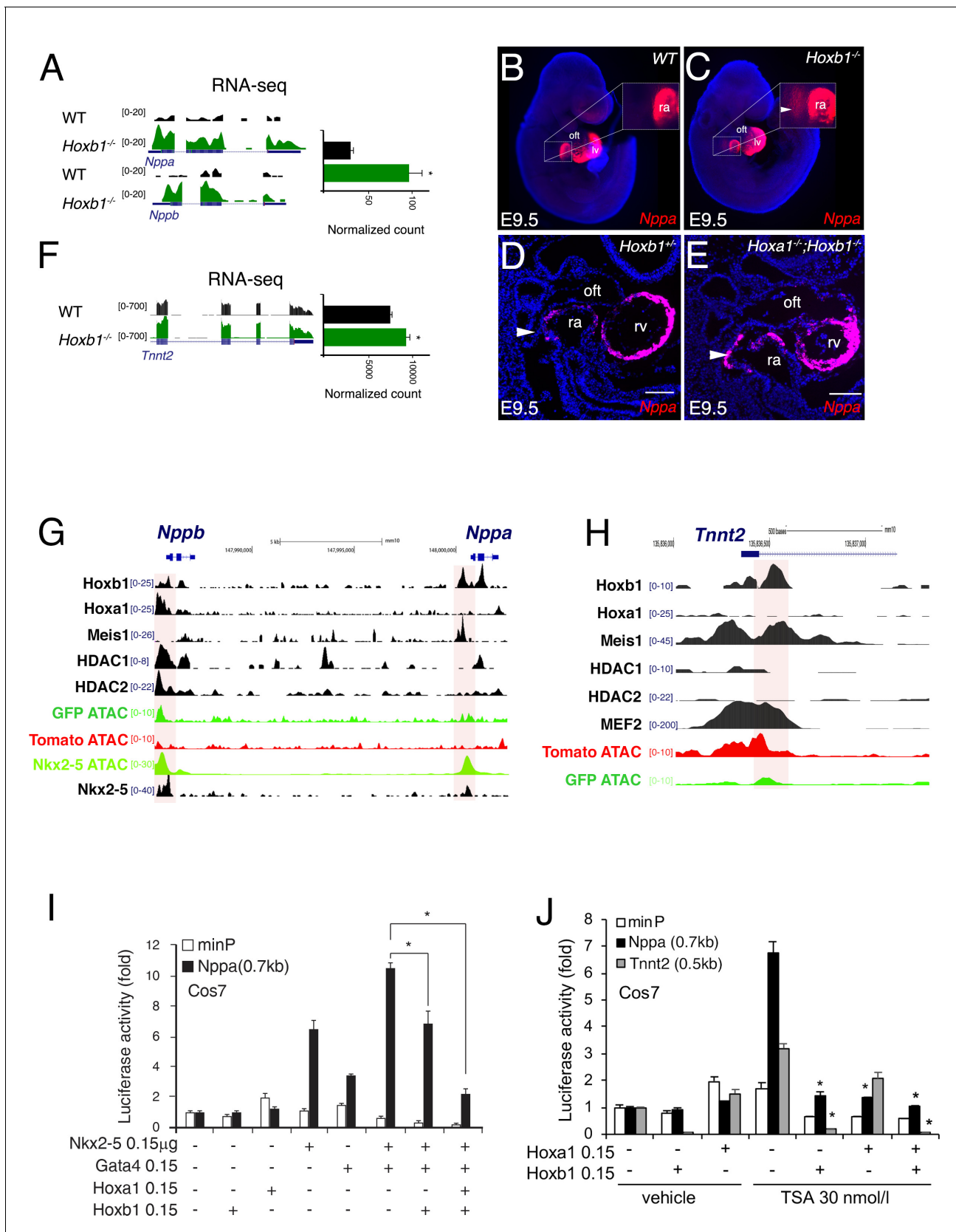


**Figure 8.** *Hoxb1* regulates cardiac differentiation through transcriptional repression of myocardial genes. (A) Browser views of *Nppa* and *Nppb* gene loci with RNA-seq profiles of *Hoxb1*<sup>-/-</sup> (green) and wild-type (WT) population (black). Data represent the merge of technical and biological replicates for Figure 8 continued on next page

## Figure 8 continued

each cell type. The y-axis scales range from 0 to 20 in normalized arbitrary units. (B,C) Whole mount RNA-FISH for *Nppa* in WT (B) and *Hoxb1*<sup>-/-</sup> (C) E9.5 embryos. Inset displays higher magnification of the posterior heart region. Nuclei are stained with Dapi. RNA-FISH on sagittal sections for *Nppa* in *Hoxb1*<sup>+/-</sup> (D) and *Hoxa1*<sup>-/-</sup>;*Hoxb1*<sup>-/-</sup> (E) at stage E9.5. (F) Browser view of *Tnnt2* locus with RNA-seq profiles of *Hoxb1*<sup>-/-</sup> (green) and wild-type (WT) population (black). Data represent the merge of technical and biological replicates for each cell type. The y-axis scales range from 0 to 700 in normalized arbitrary units. (G,H) Browser view of *Nppa*, *Nppb* (G) and *Tnnt2* (H) loci with ATAC-seq on purified cardiac cells and ChIP-seq profiles of Hoxb1, Hoxa1 (De Kumar et al., 2017), Meis1 (Losa et al., 2017), Nkx2-5 (van den Boogaard et al., 2012), Mef2 (Akerberg et al., 2019), HDAC1 and HDAC2 (Whyte et al., 2012). (I) Constructs were co-transfected with Nkx2-5, Gata4, Hoxa1 and Hoxb1 expression vectors into Cos-7 cells. Luciferase activity was determined and normalized as fold over the reporter alone (mean ± SEM, n = 3, \*p<0.05 for Nkx2-5 and Hoxb1 versus Nkx2-5, using ANOVA). (J) Luciferase reporter assays on the -633/+87 bp region of the *Nppa* promoter and the -497/+1 bp region of the *Tnnt2* promoter. Cos-7 cells co-transfected with Hoxa1 and Hoxb1 expressing vector or not were treated in the absence or presence of 30 nmol/l TSA. Bars represent mean ± SEM (n = 3). Statistical test was conducted using ANOVA (\*p<0.05 for Hoxa1, Hoxb1 and TSA treatment versus Hoxb1 or TSA treatment). oft, outflow tract; lv, left ventricle; ra, right atrium.

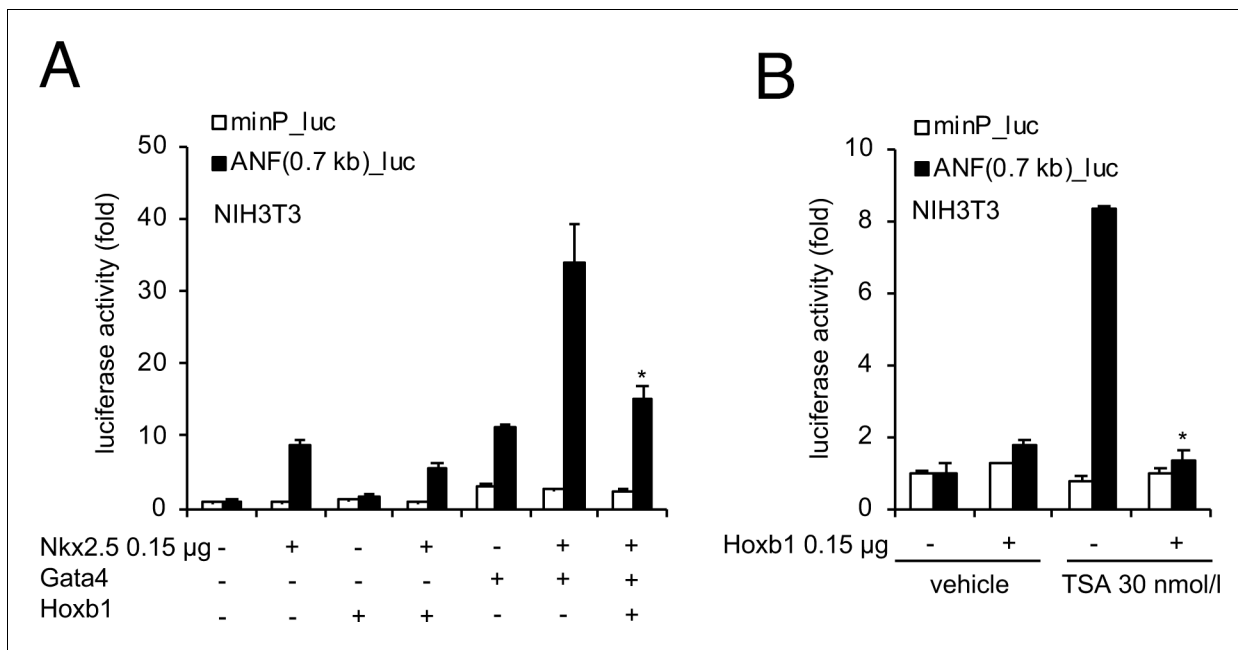


**Figure 8—figure supplement 1.** The 0.7 kb *Nppa* promoter is a functional target for Hoxb1. (A) Transient transfections were carried out with the 0.7 kb *Nppa* (ANF) promoter in NIH3T3 cells. Constructs were co-transfected with Nkx2-5, Gata4 and Hoxb1 expression vectors. Luciferase activity was determined and normalized as fold over the reporter alone (mean ± SEM, n = 3, \*p<0.05 for Nkx2-5 and Hoxb1 versus Nkx2-5, using ANOVA). (B) Luciferase reporter assays on the 0.7 kb ANF promoter in presence of TSA. NIH3T3 cells co-transfected with and without a Hoxb1 expression vector were treated in the absence or presence of 30 nmol/l TSA. Bars represent mean ± SEM (n = 3). Statistical test was conducted using ANOVA (\*p<0.05 for Hoxb1 and TSA treatment versus Hoxb1 or TSA treatment).